

Article

Accuracy Improvement of DGPS for Low-Cost Single-Frequency Receiver Using Modified Flächen Korrektur Parameter Correction

Jungbeom Kim ¹, Junesol Song ¹, Heekwon No ¹, Deokhwa Han ¹, Donguk Kim ¹,
Byungwoon Park ^{2,*} and Changdon Kee ^{1,*}

¹ School of Mechanical and Aerospace Engineering and Institute of Advanced Aerospace Technology, Seoul National University, 1 Gwanak-ro, Gwanak-gu, Seoul 08826, Korea; magicromeo@snu.ac.kr (J.K.); june85@snu.ac.kr (J.S.); nono1024@snu.ac.kr (H.N.); gksejrgkh@snu.ac.kr (D.H.); donguk319@snu.ac.kr (D.K.)

² School of Aerospace Engineering, Sejong University, 209 Neungdong-ro, Gwangjin-gu, Seoul 05006, Korea

* Correspondence: byungwoon@sejong.ac.kr (B.P.); kee@snu.ac.kr (C.K.); Tel.: +82-02-3408-4385 (B.P.); +82-02-880-1912 (C.K.)

Academic Editor: Wolfgang Kainz

Received: 17 June 2017; Accepted: 18 July 2017; Published: 20 July 2017

Abstract: A differential global positioning system (DGPS) is one of the most widely used augmentation systems for a low-cost L1 (1575.42 MHz) single-frequency GPS receiver. The positioning accuracy of a low-cost GPS receiver decreases because of the spatial decorrelation between the reference station (RS) of the DGPS and the users. Hence, a network real-time kinematic (RTK) solution is used to reduce the decorrelation error in the current DGPS system. Among the various network RTK methods, the Flächen Korrektur parameter (FKP) is used to complement the current DGPS, because its concept and system configuration are simple and the size of additional data required for the network RTK is small. The FKP was originally developed for the carrier-phase measurements of high-cost GPS receivers; thus, it should be modified to be used in the DGPS of low-cost GPS receivers. We propose an FKP-DGPS algorithm as a new augmentation method for the low-cost GPS receivers by integrating the conventional DGPS correction with the modified FKP correction to mitigate the positioning error due to the spatial decorrelation. A real-time FKP-DGPS software was developed and several real-time tests were conducted. The test results show that the positioning accuracy of the DGPS was improved by a maximum of 40%.

Keywords: differential global positioning system; Flächen Korrektur parameter; FKP-DGPS; spatial decorrelation

1. Introduction

The global positioning system (GPS), which was initially limited to military or surveying fields, has gradually been extended to ordinary industrial fields such as navigation and time synchronization. The types of GPS receivers are determined based on the performance required in each field, the price of the system, and the size of the market. For example, in the field of land surveying or bridge monitoring where high accuracy is required, high-end GPS receivers that support multi-frequency signals are used, including L1, which is the primary frequency, and L2 (1227.60 MHz), which is the secondary frequency. These receivers are used to estimate the ionospheric errors and are capable of receiving pseudorange and carrier-phase measurements. In the field of safety-of-life (SoL) service for aviation or maritime, GPS receivers that are capable of receiving L1 pseudorange and carrier-phase measurements are used. In the field of location-based service (LBS) or road systems, low-cost GPS

receivers that support the L1 single-frequency signal are used, the accuracy of which is approximately 5 m. As the price of the low-cost GPS chipsets has fallen below US one dollar and smartphones have become increasingly popular, the applications of global navigation satellite system (GNSS), such as car navigation, geo-tagging, and LBS, are likely to increase dramatically [1]. As the low-cost L1 single-frequency GPS receivers dominate most of the GPS market [2], there is a strong interest in enhancing their accuracy.

Many types of augmentation systems have been developed for low-cost GPS receivers. Among them, the differential global positioning system (DGPS) is the most representative augmentation system. DGPS services have been established worldwide. They can be divided into so-called local-area DGPS (LADGPS) services for small areas, such as a country, and wide-area DGPS (WADGPS) services for larger areas such as an entire continent or even worldwide [3]. A single reference station (RS) in a LADGPS at a known location can estimate a range of error corrections for each GPS satellite in view. These error corrections are then broadcasted to users nearby an RS. By applying these corrections to the received signals, a user can typically improve the accuracy up to a range of 1–3 m [4]. However, as the distance between the user and the RS increases, the range decorrelation increases, thus reducing the accuracy. The positioning accuracy [3,4] reduces largely because of the spatial decorrelation such as ephemeris error and ionospheric and tropospheric delays. Furthermore, if a user moves away from the RS of the LADGPS while receiving the corrections, the error due to the spatial decorrelation cannot be ignored. In this case, it is possible to receive corrections from another RS that is getting closer while moving, but the discontinuity of the position can occur.

To extend the service area using a few geosynchronous equatorial orbit (GEO) satellites and overcome the error due to the spatial decorrelation, the WADGPS has been proposed. This system is used to obtain a meter-level accuracy over a large region while using a fraction of the number of RSs. The general approach is to divide the total pseudorange error into its components and estimate the variation in each component over the entire region [5–7]. Hence, the accuracy does not depend on the proximity of the user to a single RS, such as that in the LADGPS [5]. However, the corrections regarding the ionospheric delay are broadcasted at maximum intervals of 300 s [8]. Although the intervals vary in different operating nations such as wide-area augmentation system (WAAS, USA), European geostationary navigation overlay service (EGNOS, Europe), and MTSAT satellite augmentation system (MSAS, Japan), the user needs to wait for a long time to receive all the corrections of the WADGPS. In addition, because the WADGPS has been developed for aviation, the constraint regarding the 40–50° elevation angle is not a major problem; however, it may be a major obstacle for users in urban and mountainous areas while receiving the signals from the GEO satellites. In other words, if a signal is interrupted while receiving corrections, the user needs to wait when the correction data are not being received. Hence, an effective and reasonable augmentation system is required to compensate for the error due to the spatial decorrelation even in the cases of long baselines while receiving the correction via separated communication from the LADGPS. A network real-time kinematic (RTK) solution is used to reduce the decorrelation error in a Carrier-phase DGPS system. Among the various network RTK methods, the Flächen Korrektur parameter (FKP), which is a suitable methodology to complement the current DGPS using an one-way communication environment, is also useful to complement the current LADGPS. KODGIS and NAWGIS services operated by the ASG-EUPOS in Poland are examples of systems to improve the low-cost receiver using the network RTK solution, which is very rare in other countries or infrastructures. While the KODGIS generates DGPS correction directly for the user's location based on the virtual reference station (VRS) concept, the NAWGIS generates DGPS correction for strictly defined points (the geometric centers of the station network are for northern and southern Poland) based on the VRS concept to compensate for the spatial decorrelation error of the DGPS [9,10]. To provide the service, it uses a proprietary message from the radio technical commission for maritime (RTCM) for the solution. Thus, exclusive users who made a contractor with the operator support the system. The proprietary message of the NAWGIS (message

type 59) has been recently moved to the reserved message for private use in the RTCM version 2.3, and mass market low-cost receivers such as u-blox series do not support the private message.

In this study, we propose a user-oriented FKP-DGPS algorithm as a new augmentation system by integrating the conventional LADGPS correction with the modified FKP correction. This system combines the existing LADGPS and FKP infrastructures, and subsequently, generates a new correction to be provided to the low-cost GNSS receivers based on the RTCM standard. It does not require a special infrastructure for the FKP-DGPS and follows the current standards. Thus, any LADGPS user can compensate for the spatial decorrelation error by itself. In addition to solving the spatial-decorrelation problem in the LADGPS, it can be a solution for the signal corruption of the WADGPS correction from the satellite based augmentation system (SBAS) GEO satellite. Because it is difficult to ensure a stable service for land users based on the SBAS corrections, this study focuses on the ground infrastructure that provides the LADGPS service; herein, the DGPS referred is the LADGPS. The remainder of this paper is organized as follows. Section 2 describes the spatial decorrelation of the LADGPS and introduces a method of reducing its influence using a modified FKP correction with the help of mathematical analysis. Section 3 focuses on the method of developing a real-time FKP-DGPS algorithm using the modified FKP correction; moreover, the method of applying the calculated FKP-DGPS correction to a low-cost L1 single frequency GPS receiver is presented. Section 4 shows the results of the static and dynamic user tests conducted to confirm the improvement in the accuracy obtained through the developed algorithm. Finally, the performance of the developed algorithm in determining the reduced positioning errors with sufficient coverage area is verified through the test results.

2. DGPS and FKP

2.1. DGPS and Spatial Decorrelation

GPS is a widely known navigation system providing accurate, continuous, worldwide, three-dimensional position, velocity and time information. The positioning accuracy of the low-cost L1 single-frequency GPS receivers is generally about 5 m to 10 m because many sources of possible errors reduce the positioning accuracy [5]. In the space segment, GPS satellite orbit and clock errors exist. In addition, while a signal is being transmitted from a GPS satellite to a user, the atmospheric effects such as ionospheric and tropospheric delays may alter the travel time of the GPS signal. In the user segment, multipath error and noise exist. Except for the errors induced in the user segment, other errors, which are characteristic of the spatial correlation, can be fairly eliminated using the correction from the RS of the DGPS. In other words, the RS of the DGPS, which is positioned at a known location that was previously surveyed, can estimate the errors in its GPS signals and broadcast the correction data to nearby users.

Figure 1 shows the range errors between the RS and the users considering only the atmospheric effects. Even if there are common errors in the measurements, they cannot be exactly equal because of the spatial decorrelation. As the separation of the user from the RS increases, the difference in the ionospheric and tropospheric delay between the two sites increases. Table 1 lists the different errors depending on the separation based on recent studies [11,12].

Table 1. Quantity of spatial decorrelations [12].

Delay	Average	Maximum
Ionospheric	4 m	40 m
Tropospheric	2 m	16 m
Ephemeris	<0.25 m	<0.25 m

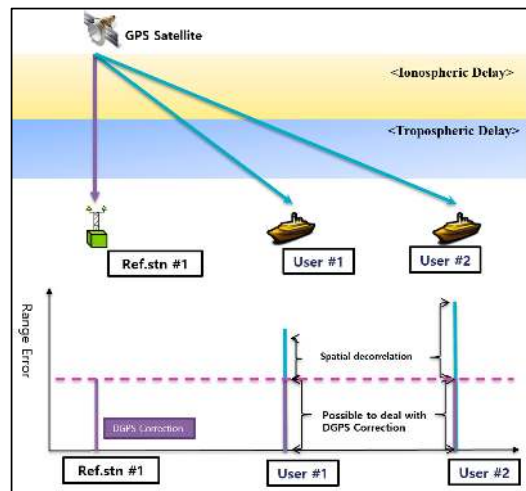


Figure 1. DGPS concept and spatial decorrelation.

The errors due to the spatial decorrelation can be expressed using the following equations. First, the pseudorange measurements of the user and RS are given below.

$$\begin{aligned}
 \rho_u^i &= \left(\bar{R}^i + \delta\bar{R}^i - \bar{R}_u \right) \cdot \bar{e}_u^i - b^i + I_u^i + T_u^i + B_u + \varepsilon_u^i \\
 \rho_u^j &= \left(\bar{R}^j + \delta\bar{R}^j - \bar{R}_u \right) \cdot \bar{e}_u^j - b^j + I_u^j + T_u^j + B_u + \varepsilon_u^j \\
 \rho_r^i &= \left(\bar{R}^i + \delta\bar{R}^i - \bar{R}_r \right) \cdot \bar{e}_r^i - b^i + I_r^i + T_r^i + B_r + \varepsilon_r^i \\
 \rho_r^j &= \left(\bar{R}^j + \delta\bar{R}^j - \bar{R}_r \right) \cdot \bar{e}_r^j - b^j + I_r^j + T_r^j + B_r + \varepsilon_r^j
 \end{aligned} \tag{1}$$

The superscripts i and j denote the i th and j th GPS satellites, respectively, and the subscripts u and r denote the user and RS, respectively. In addition, $\bar{R}, \bar{e}, b, B, I, T, \delta R$, and ε are the position, line of sight vector, satellite clock bias, receiver clock bias, ionospheric delay, tropospheric delay, ephemeris error, and noise, respectively. By subtracting between two satellites single differences (${}^i\nabla^j\rho_u, {}^i\nabla^j\rho_r$), the double-difference measurement is obtained as follows.

$$\begin{aligned}
 {}_u\Delta_r^i\nabla^j\rho &= \left[\left(\bar{R}^i + \delta\bar{R}^i \right) \cdot \bar{e}_u^i - \left(\bar{R}^j + \delta\bar{R}^j \right) \cdot \bar{e}_u^j \right] - \bar{R}_u \cdot \left(\bar{e}_u^i - \bar{e}_u^j \right) \\
 &+ \left(I_u^i - I_u^j \right) + \left(T_u^i - T_u^j \right) + {}^i\nabla^j\varepsilon_u \\
 &- \left[\left(\bar{R}^i + \delta\bar{R}^i \right) \cdot \bar{e}_r^i - \left(\bar{R}^j + \delta\bar{R}^j \right) \cdot \bar{e}_r^j \right] + \bar{R}_r \cdot \left(\bar{e}_r^i - \bar{e}_r^j \right) \\
 &- \left(I_r^i - I_r^j \right) - \left(T_r^i - T_r^j \right) - {}^i\nabla^j\varepsilon_r
 \end{aligned} \tag{2}$$

As explained previously, the measurement of the user apart from the RS includes the spatial decorrelation errors. Hence, considering the decorrelation errors ($\delta I, \delta T$), the relationship between the common errors can be expressed as follows.

$$\begin{aligned}
 I_u^i &= I_r^i + \delta I^i, T_u^i = T_r^i + \delta T^i - r \Delta_u T_{\text{model}}^i \\
 I_u^j &= I_r^j + \delta I^j, T_u^j = T_r^j + \delta T^j - r \Delta_u T_{\text{model}}^j
 \end{aligned} \tag{3}$$

where $\delta I, \delta T$ are the components of the ionospheric and tropospheric delays, respectively, due to the spatial decorrelation between the user and the RS. In addition, the subscript “model” denotes the value that is calculated using a tropospheric model. Several errors can be appropriately determined using various models such as the Klobuchar model for ionospheric delay and a simple model for the tropospheric delay. In particular, the tropospheric delay can be approximated using the model because the tropospheric refraction arises from the predictable component [13]. Hence, assuming that the user and the RS use the tropospheric model to eliminate the tropospheric error in their

measurements, the relationship of the tropospheric delay can be expressed using the above equation. Because the ephemeris error is less affected by the spatial decorrelation compared to the ionospheric and tropospheric delays, as listed in Table 1, it can be ignored in this mathematical analysis along with the noise. By substituting Equation (3) into Equation (2), we obtain the following equation.

$$\begin{aligned} {}_u\Delta_r^i \nabla^j \rho &= \bar{R}^i \cdot {}_u\Delta_r \bar{e}^i - \bar{R}^j \cdot {}_u\Delta_r \bar{e}^j - \bar{R}_u \cdot \bar{e}_u^i + \bar{R}_u \cdot \bar{e}_u^j + \bar{R}_u \cdot \bar{e}_u^i - \bar{R}_u \cdot \bar{e}_u^j \\ &+ ({}^i\nabla^j \delta T - {}_r\Delta_u^i \nabla^j T_{\text{model}}^i) + ({}^i\nabla^j \delta I) \end{aligned} \quad (4)$$

Finally, the errors due to the spatial decorrelation in the double-difference measurement are confirmed. Hence, it is reasonable to conclude that the position accuracy reduces because of the spatial decorrelation.

2.2. Network RTK and FKP

The positioning method based on the carrier-phase measurement is quite difficult because of the process of determining the integer ambiguity [14]. The spatial decorrelation affects the resolution of the integer ambiguity. Hence, many studies have been conducted on the spatial decorrelation and several network-RTK methods have been developed such as the VRS, master-auxiliary concept (MAC), and FKP.

The VRS is the most widely used augmentation system worldwide. It provides an accurate, stable, and suitable service for static users. It can be used in all receivers wherein the RTCM message is employed. Moreover, the VRS has better performance than the other methods. However, a bidirectional communication is required because the corrections are transmitted only after receiving the position of the user [15]. Therefore, there is a privacy problem and it is unsuitable for dynamic users who are moving continuously and can go anywhere. In case of a system used in a local area such as precise farming, the correction received from the starting point may be continuously valid [16]. However, the performance deterioration due to the spatial decorrelation is inevitable for the user moving away from the starting point, and the correction from a new VRS point for the current user position should be updated to compensate for the decorrelation error, thereby leading to a VRS hand-over problem.

The MAC has been developed to supplement the previously developed VRS and compensate for the drawbacks of the FKP with more accurate and stable positioning compared to the VRS and FKP. The MAC comprises a master RS and several auxiliary RSs. Each auxiliary RS sends its own measurements to the master, and the inter-station difference in the correction is used to estimate the required correction. This correction can be divided into dispersive (ionospheric) and non-dispersive (geometric) corrections for broadcast efficiency, and it can be modified for the low-cost GPS receivers. In addition, this solution can be applied with a one-way communication; thus, a user of a kinematic application can determine the position regardless of any interruption or discontinuity. However, the amount of data is somewhat high, and the method applied by the user is somewhat complicated [15].

The FKP is an “area-correction parameter” and it is one of the first methods that was developed to implement a network RTK. The FKP is used to calculate the coefficients of a polynomial surface, which models the correction difference referenced to the master station. These coefficients are horizontal gradients for the dispersive and non-dispersive errors, and are used to evaluate the error polynomial at the desired location. The user interpolates the corrections and applies them with the master station observations or corrections [15,17]. It helps broadcast coefficients that can express the error plane efficiently in a way described in Figure 2. Thus, it is suitable for broadcasting corrections. Like the MAC, this solution can be applied with a one-way communication; thus, a user of a kinematic application can determine the position regardless of any interruption or discontinuity. Although the decision made by the provider regarding the complexity of the model can influence the performance of the user, and the accuracy of the FKP is less than that of other methods, the amount of data is small; moreover, the method applied by the user is simple [15,18]. Hence, in this study, we propose a new augmentation method to improve the accuracy of the current DGPS using practical and suitable FKP corrections for all the users described above.

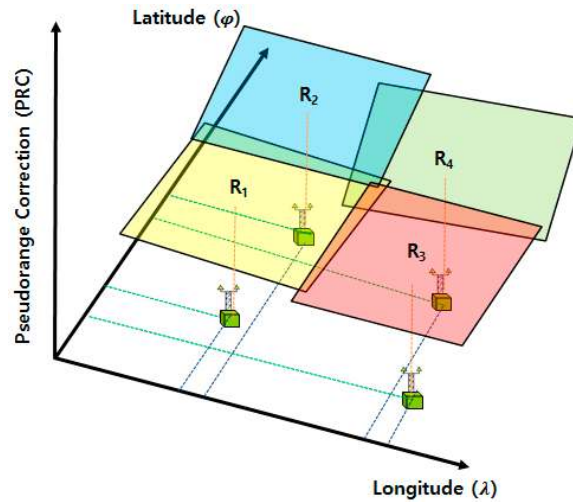


Figure 2. Linear FKP planes for four RSs [19].

The range errors due to the spatial decorrelation in the space between the two RSs can be estimated, as shown in Figure 3. In other words, the FKP RS is used to calculate the distance-dependent range errors in close proximity to itself by comparing the range errors of nearby RSs. Subsequently, it helps convert them into error surfaces and broadcast their first-order linear approximated gradients as FKP corrections. Therefore, the users can eliminate the effects of the spatial decorrelation using the FKP correction. The FKP is less accurate than the VRS and MAC because it simplifies the range errors into the first-order gradients. Nevertheless, it can be easily modified for pseudorange measurements in the low-cost L1 single-frequency GPS receiver. The parameters of the FKP correction show that the horizontal gradients are linear approximations of the geometric and ionospheric errors in the neighborhood of the RS. The geometric gradient contains the non-dispersive (ephemeris and troposphere residuals) errors whereas the ionospheric gradient contains the dispersive errors. The geographical coordinates φ_r, λ_r are the ellipsoidal coordinates of the corresponding RS and the coordinates of the user are φ, λ . The corrections can be then written as follows.

$$\begin{aligned} \delta\rho_o &= 6.37 \cdot (N_o(\varphi - \varphi_r) + E_o(\lambda - \lambda_r) \cos(\varphi_r)) \\ \delta\rho_I &= 6.37 \cdot H \cdot (N_I(\varphi - \varphi_r) + E_I(\lambda - \lambda_r) \cos(\varphi_r)) \end{aligned} \tag{5}$$

$$H = 1 + 16(0.53 - eI/\pi)^3$$

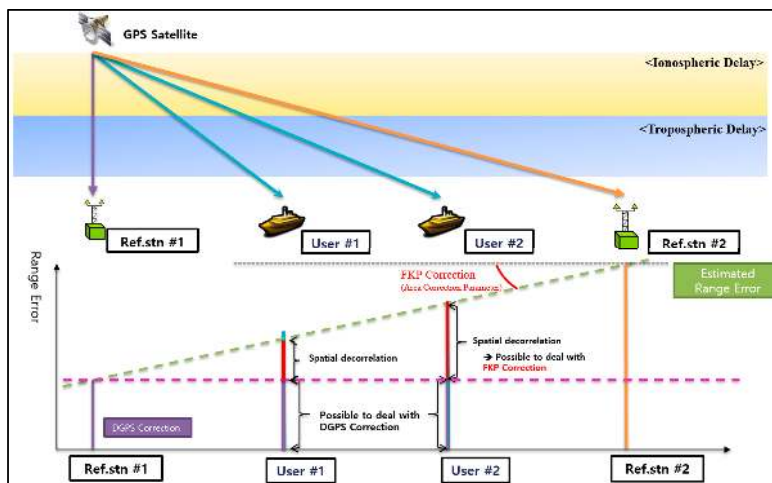


Figure 3. Broadcasted FKP correction information.

The subscripts o and I denote the components of the geometric and ionospheric signals, respectively. In addition, N, E, el are the gradients in the north–south and east–west directions and elevation angle of the satellite at the user position, respectively [20,21]. These parameters are transmitted to the user through the network transport of the RTCM via the Internet protocol (NTRIP) in the form of an RTCM version 3.1 standard message. Based on the RTCM standard document, message type 1034 contains the FKP gradients and message type 1005 contains the station coordinates [21]. Regions where the users make use of the FKP service are such as many European countries including Germany, parts of America, Korea, Japan, and Australia [22].

The ephemeris error due to the spatial decorrelation is much smaller than the tropospheric delay. Hence, the correction used for the geometric errors can be used for the tropospheric delays. In addition, the sign of the correction for the ionospheric error should be reversed for the pseudorange measurements because the correction in Equation (5) is obtained for the carrier-phase measurements. Accordingly, Equation (5) is modified as follows.

$$\delta\rho_o = \delta T_{FKP} \simeq \delta T, \delta\rho_I = -\delta I_{FKP} \simeq \delta I \quad (6)$$

The subscript FKP denotes the corrections made using the FKP messages. The residual errors due to the spatial decorrelation in Equation (4) could be then eliminated using the modified FKP corrections as follows.

$$\begin{aligned} {}_u\Delta_r^i \nabla^j \rho - & \left(\bar{R}^i \cdot {}_u\Delta_r \bar{e}^i - \bar{R}^j \cdot {}_u\Delta_r \bar{e}^j - \bar{R}_u \cdot \bar{e}_u^i + \bar{R}_u \cdot \bar{e}_u^j + \bar{R}_u \cdot \bar{e}_u^i - \bar{R}_u \cdot \bar{e}_u^j \right) \\ & = ({}^i\nabla^j \delta T - {}_r\Delta_u^i \nabla^j T_{\text{model}}^i) + ({}^i\nabla^j \delta I) \\ & \simeq ({}^i\nabla^j \delta T_{FKP} - {}_r\Delta_u^i \nabla^j T_{\text{model}}^i) + (-{}^i\nabla^j \delta I_{FKP}) \end{aligned} \quad (7)$$

3. FKP-DGPS Algorithm

3.1. RTCM Version 2.3

The development of the real-time FKP-DGPS algorithm is based on the DGPS messages, which are broadcasted in the RTCM version 2.3 format through the NTRIP. The broadcasting information in the RTCM version 2.3 contains various messages regarding the DGPS correction and network RTK. Among the various messages, the low-cost GPS receiver requires several messages such as message types 1, 2, 3, and 9 to obtain the position of the DGPS more accurately, instead of only a standalone position [23,24]. Including the u-blox receiver, which is a typical low-cost GPS receiver, the commercial low-cost L1 single-frequency GPS receivers have an interface to receive the RTCM version 2.3 messages for the DGPS. Figure 4 shows the structure of the message type 1 in the RTCM version 2.3. The structure comprises various information, such as pseudorange correction (PRC) and range-rate correction (RRC), which is expressed as pseudorange correction change rate in Figure 4, issue of data (IOD), and user differential range error (UDRE). The DGPS correction for each satellite in message type 1 is approximately 40 bits except for the parity data, and it is usually broadcasted every second. The PRC is the main information for the DGPS, and we explain the method of integrating the modified FKP corrections with the PRC information of the message type 1 in Section 3.3.

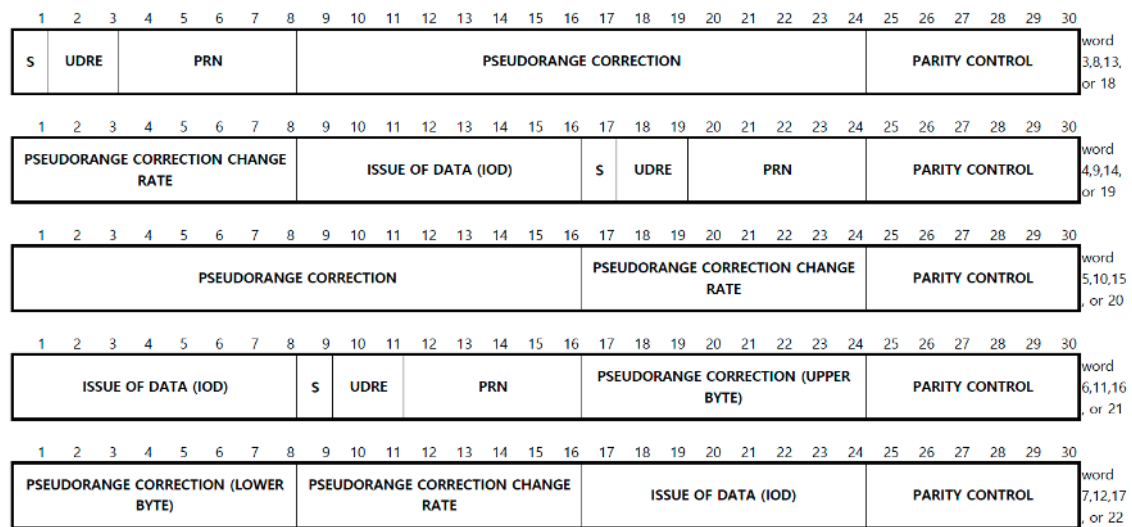


Figure 4. Structure of message type 1 in RTCM version 2.3.

3.2. RTCM Version 3.1 [21]

The development of the real-time FKP-DGPS algorithm is based on the FKP messages, which are broadcasted in the RTCM version 3.1 format through the NTRIP. The broadcasting information in the RTCM version 3.1 contains various messages regarding the GPS observations and network RTK. Among the various messages, message type 1034 contains the GPS network FKP gradient message comprising geometric and ionospheric gradients as shown in Table 2. The FKP information per satellite in the message type 1034 is approximately 66 bits except for the parity data, and it is usually broadcasted at intervals in the range of 10~15 s.

Table 2. Structure of message type 1034 in RTCM version 3.1.

Data Field	Data Type	Number of Bits
GPS Satellite ID	unsigned int6	6
GPS Issue of data ephemeris (IDOE)	bit(8)	8
N0: Geometric gradient (North)	int12	12
E0: Geometric gradient (East)	int12	12
NI: Ionospheric gradient (North)	int14	14
EI: Ionospheric gradient (East)	int14	14
Total		66

3.3. Real-Time FKP-DGPS Algorithm [25,26]

Using the modified FKP corrections, shown in Equations (5) and (6), the PRC in message type 1 of the RTCM version 2.3 can be described as follows.

$$\begin{aligned}
 PRC_{FKP-DGPS} &= PRC_{DGPS} + PRC_{FKP} \\
 PRC_{FKP} &= \delta T_{FKP} - r \Delta u T_{model} - \delta I_{FKP}
 \end{aligned}
 \tag{8}$$

In other words, we decoded the received message type 1 and integrated the PRC in the message with the modified FKP corrections using the FKP gradient information typically transmitted every 10~60 s. In addition, the tropospheric delays are generated using the Niell mapping function and Saastamoinen tropospheric zenith-delay model, which are recommended in the RTCM standard document. The integrated PRC of the FKP-DGPS is encoded in accordance with the format of the original message type 1.

Figure 5 shows the process of the real-time FKP-DGPS algorithm. First, the user and correction data are acquired such as the DGPS correction in the RTCM version 2.3 and the FKP correction data in RTCM version 3.1. Using the collected data, the tropospheric delays are generated, and the FKP corrections are calculated as explained previously using Equations (5) and (8). Finally, it is necessary to encode the generated FKP-DGPS correction in the form of message type 1 in the RTCM version 2.3 to directly apply it to the commercial low-cost L1 single-frequency GPS receiver. Thus, we can acquire the FKP-DGPS position in real-time at the output of the receiver.

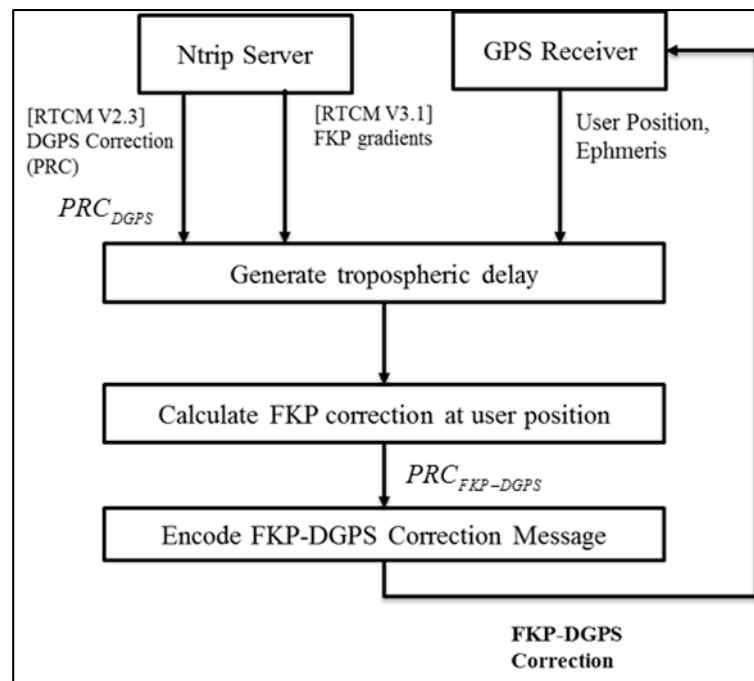


Figure 5. Flow chart of real-time FKP-DGPS algorithm.

4. Test Results

4.1. System Configuration

Currently, the GPS-related correction information is being broadcasted in Korea by various agencies such as National Geographic Information Institute (NGII), Korea Astronomy and Space Science Institute (KASSI), and National Maritime PNT Office (NMPO). Most of these services are widely used for the RSs operated by NGII. There are more than 50 RSs operated by NGII as described in Figure 6, providing various services such as VRS, MAC, FKP, and DGPS. The RSs are used to simultaneously broadcast the DGPS (mountpoint: DGPS_V2) and FKP correction (mountpoint: FKP_V31) information. Thus, several RSs located nearby the test users were selected to receive the corrections in the tests.



Figure 6. Reference Stations operated by NGII in Korea.

4.2. Preliminary Test

Before improving the accuracy in the position domain using the FKP correction, a preliminary test was conducted on the range domain and the test data were analyzed through post-processing. The data were collected for an hour (2–3 pm in local time) on 24 September 2013. As the FKP RS, YANP station was selected which is 70 km east of INCH station as user. As analyzed previously, the divergence-free hatch-filtered (N = 1000) double-differenced (DD) measurements were used and (7) can be divided into two cases such as the residual error before applying the FKP corrections as α and that after applying them as β .

$$\alpha = \Delta_r^i \nabla_j \rho - \left(\bar{R}^i \cdot_u \Delta_r \bar{e}^i - \bar{R}^j \cdot_u \Delta_r \bar{e}^j - \bar{R}_u \cdot \bar{e}_u^i + \bar{R}_u \cdot \bar{e}_u^j + \bar{R}_u \cdot \bar{e}_u^i - \bar{R}_u \cdot \bar{e}_u^j \right) \tag{9}$$

$$\beta = \alpha - \left({}^i \nabla^j \delta T_{FKP} - r \Delta_u^i \nabla^j T_{\text{model}}^i \right) + \left(-{}^i \nabla^j \delta I_{FKP} \right)$$

As shown in Figure 7, the residual errors decreased because of the positive effect of the FKP corrections. In addition, most of the range errors of each satellite were reduced by more than 0.1 m and the maximum reduced error is approximately 0.35 m on PRN #8 (the smallest elevation angle) as listed in Table 3. This is because the smaller the elevation angle, the higher is the error due to the spatial decorrelation [27].

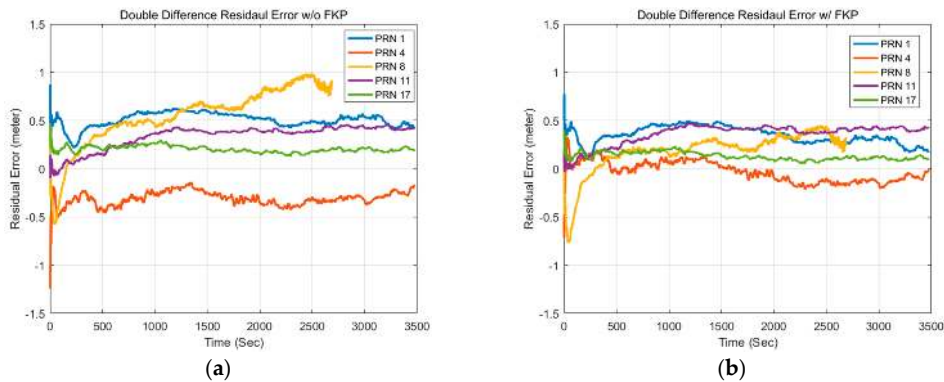


Figure 7. (a) DD residual errors without FKP correction; and (b) DD residual errors with FKP correction.

Table 3. DD residual errors without and with FKP correction.

DD Residual Errors (RMS ¹)	PRN #1	PRN #4	PRN #8	PRN #11	PRN #17
Elevation Angle	49.9°	15.9°	14.3°	30.6°	43.3°
Before Case (α)	0.51 m	0.32 m	0.63 m	0.36 m	0.21 m
After Case (β)	0.36 m	0.11 m	0.28 m	0.37 m	0.14 m

¹ Root mean square (RMS).

4.3. Static Test

To confirm the improvement in the accuracy of the DGPS of the low-cost single frequency GPS receiver using the modified FKP corrections in the position domain, static and dynamic user tests were conducted. First, the static test is introduced.

In the static test, Figure 8a shows the u-blox LEA-6T evaluation kit selected as the low-cost GPS receiver, which is one of the most popular and inexpensive commercial GPS receivers. It can be applied for the DGPS messages in the RTCM version 2.3. The static user is located at Bldg. 312 in Seoul National University in Korea. In addition, to confirm the effect of the FKP corrections corresponding to the baseline lengths which is the distance between the user and the RS, four RSs (YANP, WNJU, YOWL, and WULJ) were selected which are at distances of 50, 90, 140, and 225 km south-east of the user in sequence, as shown in Figure 8b.



Figure 8. (a) u-blox LEA-6T evaluation kit; and (b) Locations of reference stations.

The test was conducted for approximately 12 h from 4 April 2017 10:30 in local time (UTC+09). To obtain the data from the four RSs simultaneously and let the receivers operate the DGPS and FKP-DGPS, eight receivers were used as the static user. In the test, an RS receiver of Trimble NetR9 and the eight u-blox receivers were connected to a Trimble Zephyr geodetic 2 antenna as shown in Figure 9. Using the measurements from the NetR9 and Zephyr antenna, a precise position was determined. Although the geodetic antenna reduces the noise level of the u-blox receiver compared to the original patch antenna, it does not reduce the bias error due to the spatial decorrelation, which can help in distinguishing the bias error from the noise-related error. In addition, Figure 10a shows the visible satellites in the sky during the test. Figure 10b shows the position dilution of precision (PDOP). The geometry of satellites affects the positioning accuracy and the dilution factor (DOP) depends solely on the geometry. Thus, the PDOP is normally presented with the positioning results in the field of GPS error analysis [28].

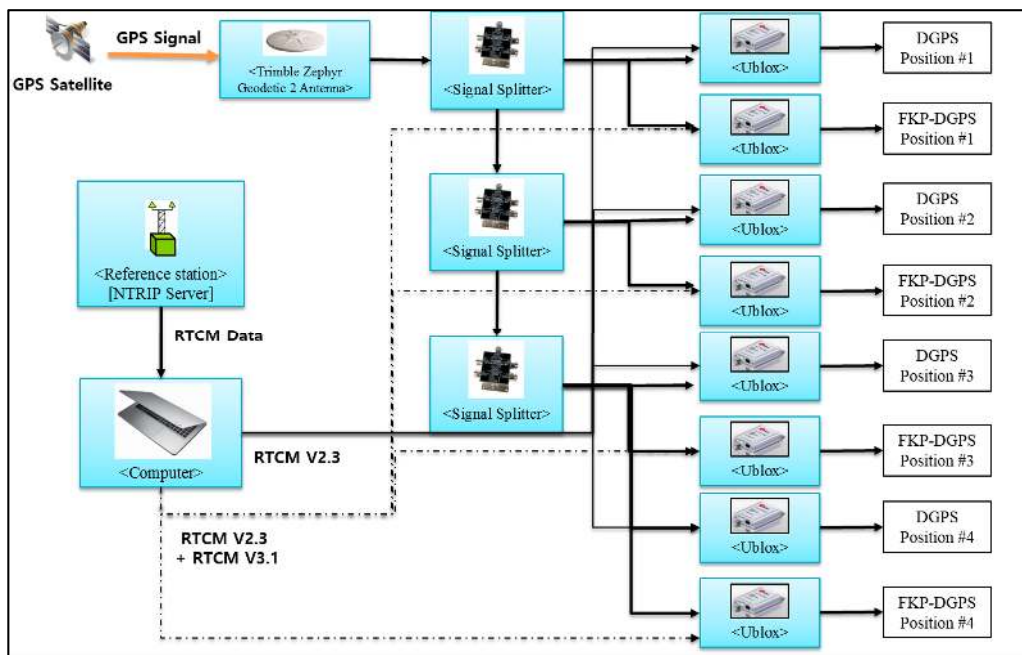


Figure 9. Configuration of the static test.

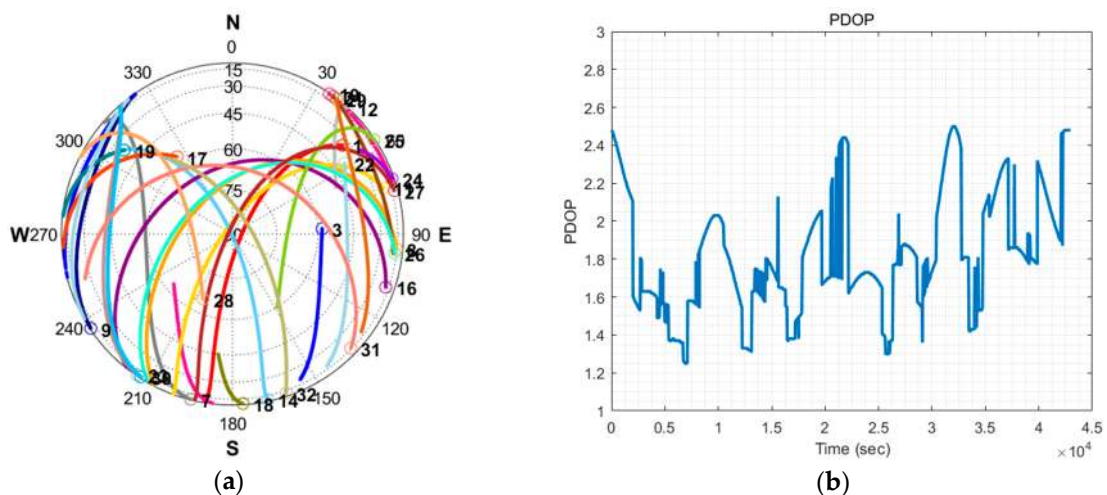


Figure 10. (a) Skyplot in static test; and (b) PDOP during static test.

Figure 11 shows the horizontal and vertical position errors of the DGPS and FKP-DGPS results of the WULJ RS, which is located farthest from the static user in the east-north-up (ENU) coordinate. It is easily confirmed that the horizontal result of the DGPS is slightly biased on the left side. However, the horizontal result of the FKP-DGPS seems unbiased, but slightly noisy. Furthermore, the positive effect of the FKP correction can be confirmed from the vertical result. The blank in the vertical results occurred when the correction data are not received from the NGII FKP server because of the server-side problem. The data in the blank are excluded from the analysis.

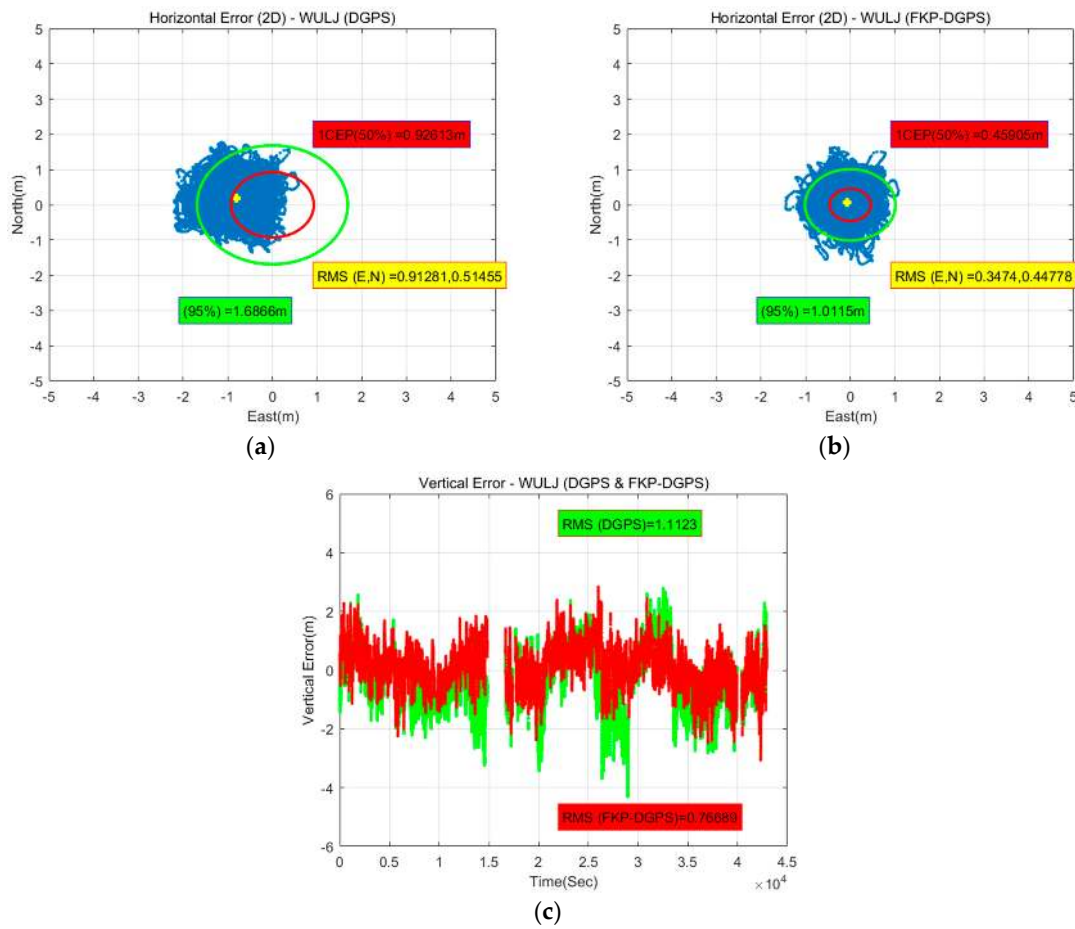


Figure 11. (a) DGPS horizontal error (WULJ); (b) FKP-DGPS horizontal error (WULJ); and (c) FKP-DGPS and DGPS vertical errors (WULJ).

Figure 12 shows the reason for the bias in the horizontal result of the DGPS on the west side. Considering the rotation of the Earth, the appearance of satellites is in the east-west direction. Moreover, satellites with low elevation angles more significantly affect positioning results. In Figure 12, it is assumed that the west direction is positive, and the GPS satellite has low elevation angle. If δ_u, δ_r are the measurement errors of the user and RS, respectively, and δ_r is equal to the correction from the DGPS RS, the residual error of the user after applying the correction from the DGPS RS can be positive, implying that the positioning error lies in the west direction. Figure 12a shows the case wherein the GPS satellite is on the east side of the user and RS. Figure 12b shows the case wherein the GPS satellite is on the west side of the user and RS.

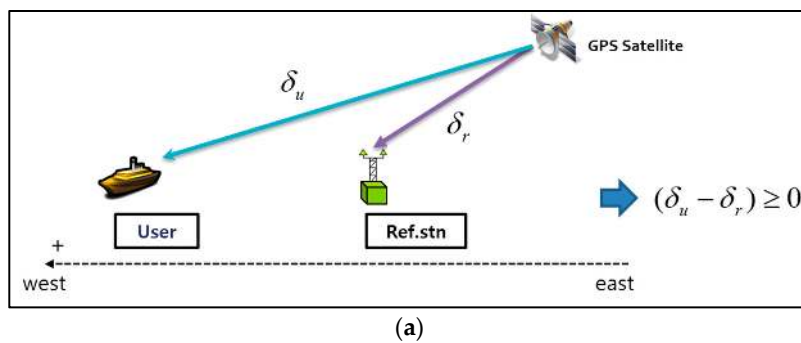


Figure 12. Cont.

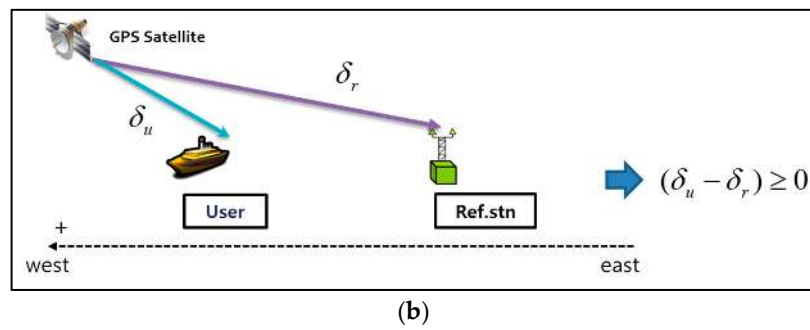


Figure 12. (a) case I—GPS satellite is on the east side of user and RS; and (b) case II—GPS satellite is on the west side of user and RS.

Tables 4 and 5 present the detailed numerical results including the results of other stations. The results show that the FKP-DGPS has more accurate positioning accuracy than the DGPS. With the increase in the baseline length, the effect of the FKP correction on the errors due to the spatial decorrelation increases with respect to the positioning accuracy. Thus, in cases of the FKP-DGPS, the improvements of the 95% horizontal accuracy of all stations are 3%, 18%, 26%, and 40% for the corresponding baseline lengths of the RSs compared to the accuracy of the DGPS. In particular, the error components of the east direction are visibly reduced when the FKP-DGPS is applied, which were large when the corrections were used from an RS far apart from the user in the east direction of DGPS. Based on the statistics in Tables 4 and 5, Figure 13a shows the 95% horizontal and vertical results corresponding to the baseline lengths. In addition, Figure 13b shows the RMS errors in the north, east, and downward directions. In Figure 13, the dashed line indicates the FKP-DGPS and the solid line indicates the DGPS. The results show that the accuracies of the FKP-DGPS remain largely constant even if the baseline lengths increase. The valid baseline length of the FKP correction for the pseudorange measurements is clearly above 200 km.

Table 4. Horizontal errors corresponding to baseline lengths.

Horizontal		YANP (50 km)	WNJU (90 km)	YOWL (140 km)	WULJ (225 km)
50% Accuracy ¹	DGPS	0.40 m	0.57 m	0.71 m	0.93 m
	FKP-DGPS	0.44 m	0.42 m	0.43 m	0.46 m
95% Accuracy	DGPS	1.05 m	1.18 m	1.34 m	1.69 m
	FKP-DGPS	1.02 m	0.97 m	0.99 m	1.01 m
RMS ² (North)	DGPS	0.43 m	0.45 m	0.50 m	0.52 m
	FKP-DGPS	0.45 m	0.42 m	0.45 m	0.45 m
RMS (East)	DGPS	0.41 m	0.51 m	0.65 m	0.91 m
	FKP-DGPS	0.33 m	0.32 m	0.32 m	0.35 m

¹ Circular error probability (CEP), ² Root mean square (RMS).

Table 5. Vertical errors corresponding to baseline lengths.

Vertical		YANP (50 km)	WNJU (90 km)	YOWL (140 km)	WULJ (225 km)
50% Accuracy	DGPS	0.52 m	0.56 m	0.57 m	0.80 m
	FKP-DGPS	0.54 m	0.55 m	0.47 m	0.51 m
95% Accuracy	DGPS	1.51 m	1.60 m	1.66 m	2.15 m
	FKP-DGPS	1.68 m	1.60 m	1.41 m	1.50 m
RMS	DGPS	0.77 m	0.83 m	0.85 m	1.11 m
	FKP-DGPS	0.84 m	0.81 m	0.71 m	0.77 m

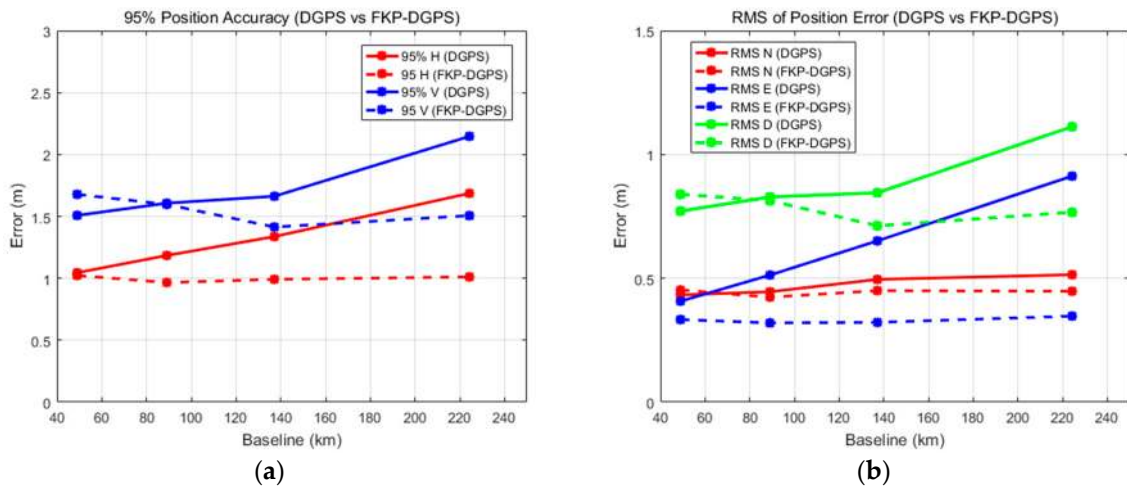


Figure 13. (a) 95% position accuracies corresponding to baseline lengths; and (b) RMS errors in north, east, downward directions corresponding to baseline lengths.

An additional test was conducted to compare the performance of the user-oriented FKP-DGPS with those of other alternatives, such as SBAS or VRS-DGPS. The configuration of the additional test is largely similar to that of the static test; the u-blox LEA-6T evaluation kit is used, and the user is located at Bldg. 312 in Seoul National University. Figure 14a shows the visible satellites in the sky during the test. Figure 14b shows the PDOP. The test was conducted for approximately 3 h from 1 July 2017 13:30 in local time (UTC+09). For the SBAS test, PRN 137 satellite of MSAS was used, which is observed at the elevation of 43° and the azimuth of 151° in Korea. For the VRS-DGPS test, we need an assumption on the dynamic user and its situation to compare the performance with VRS-DGPS, because there is no infrastructure for VRS-DGPS in Korea.

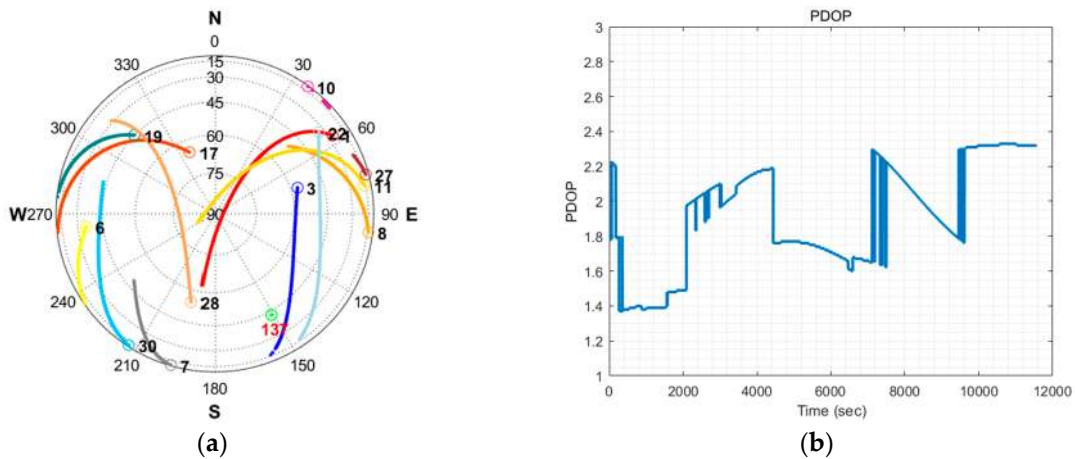


Figure 14. (a) Skyplot in additional test; and (b) PDOP during additional test.

The SBAS mode of the U-blox receiver had been set to be enabled via the u-center program. Once the configuration was set to the SBAS mode, the rover can apply the augmentation message to generate the range correction appropriate to the rover's real-time position, because the same SBAS message is broadcast to all the users in the service area regardless their location.

On the other hand, a generic VRS system provides the rover's proper correction only after it got the rover's approximate position. Moreover, a VRS user without multi-channel datalinks to nearby VRSs might experience performance degradation or discontinuity due to the absence of the correction during the handover from the previous VRS to a new one. Assuming a user who left

from WULJ and arrived at Seoul without updating its real-time position because of privacy problem or RS handover issue, the static DGPS accuracy using WULJ correction is equivalent to the VRS-DGPS accuracy of the rover at Seoul, because its VRS was not changed from the initial VRS, WULJ, through the entire journey.

In general, the SBAS has much wider coverage, but it has similar or lower positioning accuracy than the local area DGPS whose coverage is within 150 km [29]. Figure 15 shows the horizontal and vertical position errors of the SBAS, DGPS and FKP-DGPS results in the east-north-up (ENU) coordinate. In this test, the DGPS show the position error of the user of the previous VRS-DGPS assumption at Seoul, wherein the correction from the WULJ RS is used. We can easily confirm that the horizontal and vertical results of the FKP-DGPS are much better than those of the SBAS and DGPS. Table 6 lists the detailed numerical results.

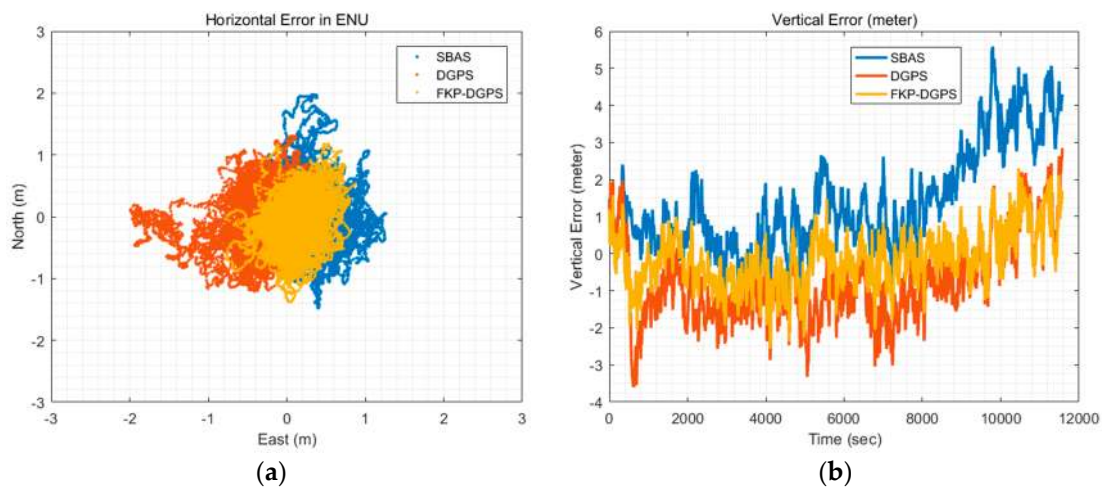


Figure 15. (a) Horizontal Error (SBAS, DGPS, and FKP-DGPS); and (b) Vertical Error (SBAS, DGPS, and FKP-DGPS).

Table 6. Position accuracies (SBAS, DGPS, and FKP-DGPS).

		SBAS	DGPS	FKP-DGPS
50% Accuracy	Horizontal	0.62 m	0.63 m	0.43 m
	Vertical	1.06 m	1.16 m	0.53 m
95% Accuracy	Horizontal	1.17 m	1.46 m	0.87 m
	Vertical	4.23 m	2.35 m	1.51 m
RMS	North	0.54 m	0.50 m	0.42 m
	East	0.49 m	0.59 m	0.29 m
	Vertical	1.98 m	1.37 m	0.77 m

4.4. Dynamic Test

Using the developed real-time FKP-DGPS software, we conducted a dynamic test to verify the feasibility of the FKP corrections for the dynamic user. The configuration of the dynamic test is largely similar to that of the static test. The u-blox LEA-6T evaluation kit is selected as the low-cost GPS receiver. Moreover, a Trimble zephyr model 2 antenna was used as the antenna. In the dynamic test, four RSs (YANP, WNJU, YOWL, and WULJ) were selected located at distances of 50, 90, 140, and 225 km south-east of the user in sequence. The dynamic test system was implemented in a land vehicle as shown in Figure 16c, which was driven inside the parking lot of Seoul Grand Park, as shown in Figure 16a. The blue line describes the trajectory of the dynamic user. The test was conducted for

approximately 25 min from 25 May 2017 15:00 in local time (UTC+09). Figure 16b,d show the visible satellites in the sky and PDOP during the test.

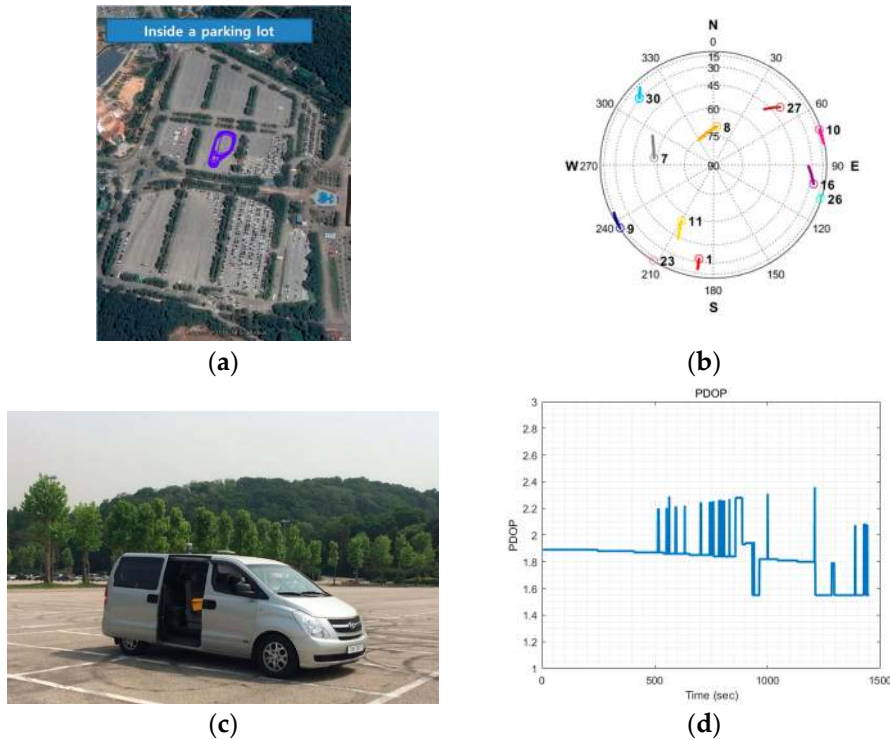


Figure 16. (a) Location of dynamic test; (b) Skyplot in dynamic test; (c) Land vehicle as dynamic user; and (d) PDOP during static test.

Figure 17 shows the horizontal and vertical position errors of the DGPS and FKP-DGPS of the WULJ RS, which is the farthest from the static user, in the ENU coordinate compared to the reference positions obtained using the Trimble NetR9 receiver with post-processing Trimble Business Center (TBC) software. The results are similar to the static test results. We can easily confirm that the horizontal result of the DGPS is slightly biased to the west side, whereas the FKP-DGPS obtains a more accurate horizontal positioning than the DGPS. Tables 7 and 8 list the detailed numerical results along with the results of other stations.

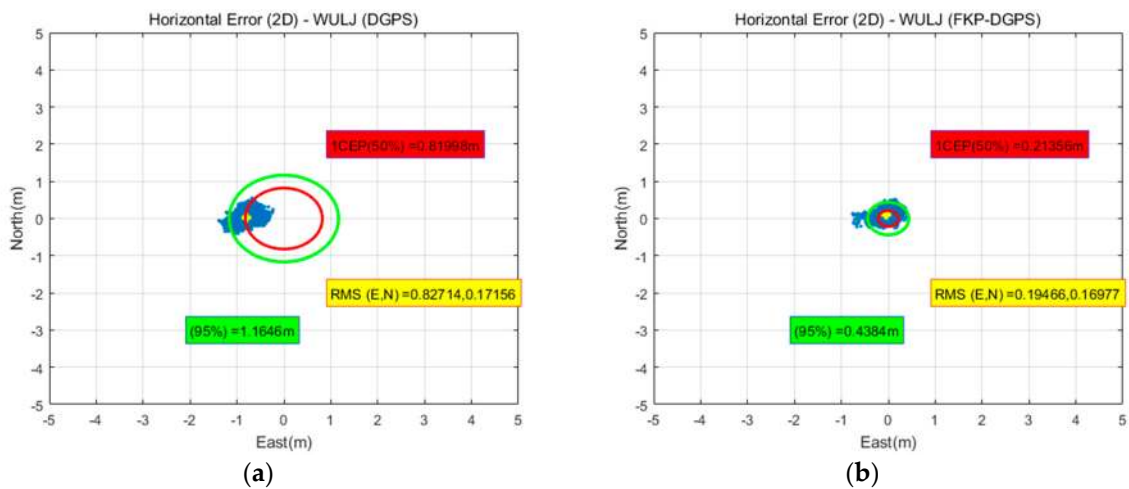


Figure 17. Cont.

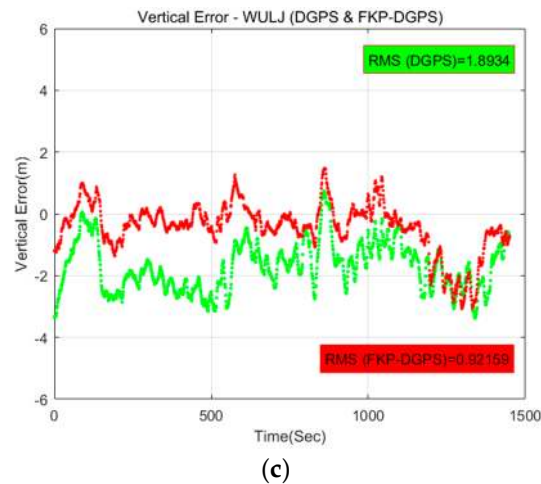


Figure 17. (a) DGPS horizontal error (WULJ); (b) FKP-DGPS horizontal error (WULJ); and (c) FKP-DGPS and DGPS vertical errors (WULJ).

Table 7. Horizontal errors corresponding to baseline lengths.

Horizontal		YANP (50 km)	WNJU (90 km)	YOWL (140 km)	WULJ (225 km)
50% Accuracy	DGPS	0.28 m	0.40 m	0.59 m	0.82 m
	FKP-DGPS	0.20 m	0.26 m	0.25 m	0.21 m
95% Accuracy	DGPS	0.49 m	0.79 m	0.81 m	1.16 m
	FKP-DGPS	0.40 m	0.54 m	0.44 m	0.44 m
RMS (North)	DGPS	0.22 m	0.22 m	0.22 m	0.17 m
	FKP-DGPS	0.18 m	0.22 m	0.22 m	0.17 m
RMS (East)	DGPS	0.21 m	0.41 m	0.56 m	0.83 m
	FKP-DGPS	0.15 m	0.25 m	0.17 m	0.19 m

Table 8. Vertical errors corresponding to baseline lengths.

Vertical		YANP (50 km)	WNJU (90 km)	YOWL (140 km)	WULJ (225 km)
50% Accuracy	DGPS	0.33 m	0.62 m	0.94 m	1.74 m
	FKP-DGPS	0.44 m	0.71 m	0.82 m	0.45 m
95% Accuracy	DGPS	1.19 m	2.20 m	1.93 m	2.88 m
	FKP-DGPS	1.30 m	2.35 m	2.02 m	2.23 m
RMS	DGPS	0.58 m	1.06 m	1.10 m	1.89 m
	FKP-DGPS	0.67 m	1.14 m	1.08 m	0.92 m

Like the static test, the FKP-DGPS has more accurate positioning accuracy than the DGPS for most of the results because of the compensate error factors due to the spatial decorrelation. Thus, in the cases of the FKP-DGPS, the improvements of the 95% horizontal accuracy of all stations are 18%, 32%, 46%, and 62% for the corresponding baseline lengths of the RSs compared to the accuracy of the DGPS. Although it is not clear to show the vertical accuracy improvement via the FKP-DGPS in a short-time period of the dynamic test, the error components of the east have definitely reduced. Figure 18a shows the 95% horizontal and vertical error tendency to the baseline length. Figure 18b describes the RMS of the error for each direction based on the result of Tables 7 and 8. In Figure 18, the dashed lines indicate the FKP-DGPS and the solid lines indicate the DGPS. From these figures, we can confirm

that the FKP-DGPS can significantly contribute to the reduction in the spatial decorrelation effect in the position-domain and the improvement in the position accuracy.

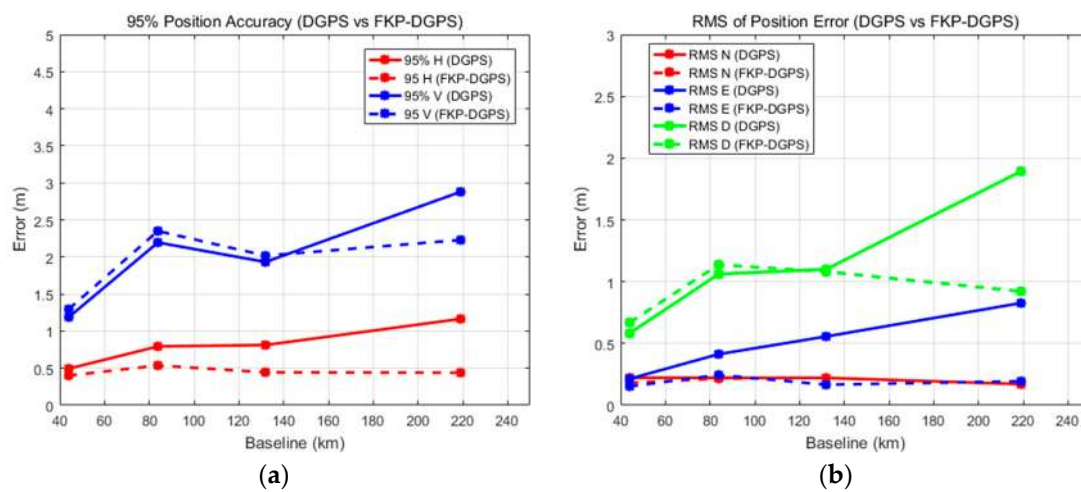


Figure 18. (a) 95% position accuracies corresponding to baseline lengths; and (b) RMS errors in north, east, and downward directions corresponding to baseline lengths.

5. Conclusions

In this study, we suggested a real-time user-oriented FKP-DGPS algorithm as a new augmentation method to improve the positioning accuracy of the DGPS. While the DGPS is the most popular augmentation system for a low-cost L1 single-frequency GPS receiver, the FKP is originally used for carrier-phase-based positioning to reduce the spatial decorrelation. To use the FKP method to improve the current DGPS accuracy without implementing a unique infrastructure for the service, we modified the FKP correction for the low-cost GPS receiver. To implement the user-oriented method to real-world applications, we combined the DGPS correction from the current DGPS server and the FKP correction from the current network RTK server operated by the NGII, and then provided the modified correction in the format of the message type 1 in the RTCM version 2.3. To verify its effect, mathematical and preliminary test-based analyses have been conducted before developing the real-time FKP-DGPS software. The preliminary-test results show that the DD residual errors with the FKP correction are less compared to those without the FKP correction. After identifying its positive effect through the analyses, the FKP-DGPS software was developed in visual C++ and several static and dynamic tests were conducted to improve the accuracy of the DGPS using the modified FKP correction. From the test results, we can confirm the improvement in the positioning accuracy of the DGPS and the positive effect of the modified FKP corrections. In the static test, compared to the accuracy of the DGPS, the improvements of the 95% horizontal accuracy of all the stations are found to be 3%, 18%, 26%, and 40% for baseline lengths of 50, 90, 140, and 225 km, respectively, which are located along the south-east direction with respect to the static user. Furthermore, the improvements in the vertical accuracy have been identified. From the dynamic test, it is difficult to identify the improvements in the vertical accuracy because the test was conducted for a short period. Nevertheless, compared to the accuracy of the DGPS, the improvements of the 95% horizontal accuracy of all the stations are 18%, 32%, 46%, and 62% for the corresponding baseline lengths. The results of the additional test show the FKP-DGPS has better performance rather than the SBAS. Hence, the new real-time FKP-DGPS algorithm is expected to exploit many applications used in our daily lives such as smartphone, car navigation, and Internet of things (IoT) devices.

Acknowledgments: This research was supported by a grant (17CTAP-C129724-01) from Technology Advancement Research Program funded by the Ministry of Land, Infrastructure, and Transport of Korean government, contracted through SNU-IAMD at the Seoul National University.

Author Contributions: All the authors have contributed to the presented work. Jungbeom Kim suggested the original algorithm of the FKP-DGPS and validated it through data processing and analysis. Changdon Kee and Byungwoon Park provided valuable comments and critical feedback regarding the algorithm. Byungwoon Park supervised its development and the direction of the research. Junesol Song and Heekwon No provided intuitive insights regarding the basic principle of the algorithm. Deokhwa Han and Donguk Kim helped in conducting the test program. All authors participated in formulating the idea and in discussing the proposed approach and results. All authors read and approved the final manuscript.

Conflicts of Interest: The authors declare no conflict of interest.

References

1. Yoon, D.; Kee, C.; Seo, J.; Park, B. Position Accuracy Improvement by Implementing the DGNSS-CP Algorithm in Smartphones. *Sensors* **2016**, *16*, 910. [CrossRef] [PubMed]
2. European GNSS Agency. *GNSS Market Report Issue 3*; European GNSS Agency: Prague, Czech Republic, 2013; pp. 7–10.
3. Retscher, G. Analysis of the System Performance of LADGPS and WADGPS Services in Europe. *J. Geospatial Eng.* **2011**, *3*, 97–107.
4. Kee, C.; Parkinson, B.W. Wide Area Differential GPS (WADGPS): Future Navigation System. *IEEE Trans. Aerosp. Electron. Syst.* **1996**, *32*, 795–808. [CrossRef]
5. Cosentino, R.J.; Diggle, D.W.; Haag, M.U.; Hegarty, C.J.; Milbert, D.; Nagle, J. Differential GPS. In *Understanding GPS Principles and Application*, 2nd ed.; Kaplan, E.D., Hegarty, C.J., Eds.; Artech House: Boston, MA, USA, 2005; pp. 379–454.
6. Brown, A. Extended Differential GPS. *J. Inst. Navig.* **1989**, *36*, 265–286. [CrossRef]
7. Kee, C.; Parkinson, B.W.; Axelrad, P. Wide Area Differential GPS. *J. Inst. Navig.* **1991**, *38*, 123–145. [CrossRef]
8. Wide-Area Augmentation System Performance Analysis Report (#8). Available online: <http://www.nstb.tc.faa.gov/reports/waaspan8.pdf> (accessed on 19 July 2017).
9. KODGIS and NAWGIS Services (ASG-EUPOS). Available online: http://www.asgeupos.pl/index.php?wpg_type=serv&sub=kodgis (accessed on 2 July 2017).
10. Performance of Real-Time Network Code DGPS Services of ASG-EUPOS in North-Eastern Poland. Available online: http://www.uwm.edu.pl/wnt/technicalsc/tech_17_3/b01.pdf (accessed on 13 July 2017).
11. Sabatini, R.; Palmerini, G.B. Differential GPS. Available online: <http://www.worldcat.org/title/differential-global-positioning-system-dgps-for-flight-testing/oclc/303405673> (accessed on 30 April 2017).
12. Park, B. A Study on Reducing Temporal and Spatial Decorrelation Effect in GNSS Augmentation System: Consideration of the Correction Message Standardization. Ph.D. Thesis, Seoul National University, Seoul, Korea, February 2008.
13. Spilker, J.J. Tropospheric Effects on GPS. In *Global Positioning System: Theory and Application*; Parkinson, B.W., Spilker, J.J., Eds.; AIAA: Washington, DC, USA, 1996; pp. 517–546.
14. Crassidis, J.L.; Markley, F.L.; Lightsey, E.G. Global Positioning System Integer Ambiguity Resolution without Attitude Knowledge. *J. Guid. Control Dyn.* **1999**, *22*, 212–218. [CrossRef]
15. Park, B.; Kee, C. The Compact Network RTK Method: An Effective Solution to Reduce GNSS Temporal and Spatial Decorrelation Error. *J. Navig.* **2010**, *63*, 343–362. [CrossRef]
16. Dabove, P.; Manzano, A.M. GPS mass-market receivers for precise farming. In Proceedings of the 2014 IEEE/ION Position, Location and Navigation Symposium—PLANS 2014, Monterey, CA, USA, 5–8 May 2014; pp. 470–477.
17. Wübbena, G.; Bagge, A.; Schmitz, M. RTK Networks based on Geo++@GNSMART – Concepts, Implementation, Results. Available online: https://www.researchgate.net/publication/242719411_RTK_Networks_based_on_Geo_R_GNSMART_-_Concepts_Implementation_Results (accessed on 13 May 2017).
18. Petovello, M.; Dabove, P.; Agostino, M.D. GNSS Solutions: Network RTK and Reference Station Configuration. Available online: http://www.insidegnss.com/auto/IGM_novdec11-Solutions.pdf (accessed on 19 May 2017).
19. Wübbena, G.; Bagge, A.; Schmitz, M. Network-Based Techniques for RTK Applications. Available online: http://www.geopp.de/pdf/gpsjin01_p.pdf (accessed on 4 May 2017).
20. Wübbena, G.; Bagge, A. RTCM Message Type 59- FKP for Transmission of FKP. Available online: <http://www.geopp.com/pdf/geopp-rtcm-fkp59.pdf> (accessed on 4 May 2017).

21. RTCM Special Committee No. 104. RTCM Standard 10403.1. *Radio Technical Commission for Maritime Services*; RTCM Special Committee: Arlington, VA, USA, July 2011; pp. 3:78–3:83.
22. GNSMART References. Available online: <http://www.geopp.de/the-company/references/> (accessed on 2 May 2017).
23. RTCM Standard 10402.3. *Radio Technical Commission for Maritime Services*. Available online: <http://www.rtcn.org/differential-global-navigation-satellite--dgnss--standards.html> (accessed on 18 July 2017).
24. Kaźmierczak, R.; Grunwald, G.; Bakuła, M. The use of RTCM 2.X Dekoder Software for Analyses of KODGIS and NAWGIS Services of the ASG-EUPOS SYSTEM. *J. Tech. Sci. Univ. Warmia Mazury Olsztyn* **2011**, *14*, 229–243.
25. Kim, J. Improvement of DGPS Positioning Accuracy using FKP Correction Message. Master's Thesis, Seoul National University, Seoul, Korea, August 2014.
26. Kim, J.; Song, J.; No, H.; Kee, C. Feasibility Analysis of Real-Time FKP-DGPS Algorithm for L1 Single-Frequency GPS Receiver in Korea. In Proceedings of the ION 2015 Pacific PNT Meeting, Honolulu, HI, USA, 20–23 April 2015.
27. Zhang, Q.; Antoniou, M.; Chang, W.; Cherniakov, M. Spatial Decorrelation in GNSS-Based SAR Coherent Change Detection. *IEEE Trans. Geosci. Remote Sensing* **2015**, *53*, 219–228. [[CrossRef](#)]
28. Parkinson, B.W. GPS Error Analysis. In *Global Positioning System: Theory and Application*; Parkinson, B.W., Spilker, J.J., Eds.; AIAA: Washington, DC, USA, 1996; pp. 469–483.
29. GNSS Augmentation (Navipedia, ESA). Available online: http://www.navipedia.net/index.php/GNSS_Augmentation (accessed on 3 July 2017).



© 2017 by the authors. Licensee MDPI, Basel, Switzerland. This article is an open access article distributed under the terms and conditions of the Creative Commons Attribution (CC BY) license (<http://creativecommons.org/licenses/by/4.0/>).